

## The First Proton-Conducting Metallic Ion-Radical Salts\*\*

Akane Akutsu-Sato, Hiroki Akutsu, Scott S. Turner, Peter Day,\* Michael R. Probert, Judith A. K. Howard, Tomoyuki Akutagawa, Sadamu Takeda, Takayoshi Nakamura, and Takehiko Mori

Metallic materials that also conduct protons are being sought because of their potential as components in solid-state electrochemical devices, such as batteries and fuel cells.<sup>[1]</sup> To date, the search has concentrated mainly on purely inorganic materials, and in particular continuous lattice oxides. In fact, there is a clear lack of candidates among electronically conducting organic molecular crystals, despite the existence of proton-conducting polymers, such as perfluorinated Nafion. Recently a 2,2'-[2,5-cyclohexadiene-1,4-diylidene]-bis(propanedinitrile) (TCNQ) charge transfer complex of benzimidazolyl-benzimidazole was shown to exhibit coupled protonic and electronic conductivity, and a TCNQ complex of 1,4-diazabicyclo[2.2.2]octane also exhibited proton transfer.<sup>[2]</sup> Herein we report what we believe to be the first molecular ion-radical salts that are metallic conductors at room temperature, and also show a high proton conductivity. We provide evidence that the mobility of both protons and electrons is

[\*] Dr. A. Akutsu-Sato, Dr. H. Akutsu, Dr. S. S. Turner, Prof. P. Day  
Davy–Faraday Research Laboratory (DFRL)  
Royal Institution of Great Britain  
21 Albemarle Street, London, W1S 4BS (United Kingdom)  
Fax: (+44) 20-7629-3569  
E-mail: pday@ri.ac.uk

Dr. S. S. Turner  
School of Biological and Chemical Sciences  
Department of Chemistry, University of Exeter  
Exeter, EX4 4QD (United Kingdom)

M. R. Probert, Prof. J. A. K. Howard  
Department of Chemistry, University of Durham  
South Road, Durham, DH1 3LE (United Kingdom)

Dr. H. Akutsu  
Graduate School of Material Science  
University of Hyogo, Hyogo, 678-1297 (Japan)

Dr. A. Akutsu-Sato, Prof. T. Mori  
Department of Organic and Polymeric Materials  
Tokyo Institute of Technology  
O-okayama, Megaru-ku, Tokyo, 113-0033 (Japan)

Prof. T. Akutagawa, Prof. T. Nakamura  
Research Institute for Electronic Science  
Hokkaido University, Sapporo, 060-0812 (Japan)

Prof. S. Takeda  
Division of Chemistry, Graduate School of Science  
Hokkaido University, Sapporo, 060-0812 (Japan)

[\*\*] This work was supported by the Engineering and Physical Sciences Research Council, EPSRC, (UK), and Monbukagakusho (Japanese Ministry for Education, Culture, Sports, Science and Technology). H.A. and A.A.-S. wish to thank the Japanese Society for the Promotion of Science (JSPS) for postdoctoral fellowships at the DFRL. JAKH thanks the EPSRC for a Senior Research Fellowship.

high in these lattices because of a unique crystal structure consisting of layers of organic donor molecules interleaved with arrays of stacked crown ether molecules. The crown ether molecules form “pipes” filled with water molecules. The crystal structure, resolved from X-ray data recorded at 30 K,<sup>[3]</sup> gives strong indication of a hydrogen-bonding network, which gives rise to the protonic conductivity.

The series of cation-radical salts (BEDT-TTF)<sub>4</sub>[(Cat)M(C<sub>2</sub>O<sub>4</sub>)<sub>3</sub>]G, where BEDT-TTF = bis(ethylenedithio)tetrathiafulvalene, has proven to be an exceptionally fruitful source of different collective electronic ground states, promoted by the ease with which the monocation Cat, 3d metal M<sup>3+</sup>, and neutral guest molecule G can be varied. Thus we found the first examples of paramagnetic superconductors (Cat = H<sub>3</sub>O<sup>+</sup>; M = Cr, Fe; G = PhCN, PhNO<sub>2</sub>)<sup>[4]</sup> and the first case of polymorphism, in the whole realm of solid-state chemistry, that arose from different spatial distributions of chiral enantiomers [M(C<sub>2</sub>O<sub>4</sub>)<sub>3</sub>]<sup>3-</sup> in a racemic lattice.<sup>[5]</sup> By inserting asymmetrically substituted aromatic G molecules in cavities within the anion sublattice, it has also been possible to synthesize unique conducting salts containing a superlattice of two different packing types ( $\alpha$  and  $\beta'$ ) of the BEDT-TTF cations.<sup>[6]</sup> The present salts also contain superlattices of cation layers but, instead of being made up from two different arrangements of the BEDT-TTF molecules, they consist of BEDT-TTF and crown ether molecules that incorporate both H<sub>2</sub>O and H<sub>3</sub>O<sup>+</sup> or NH<sub>4</sub><sup>+</sup> ions.

$\beta''$ -(BEDT-TTF)<sub>4</sub>[(Cat)M<sup>III</sup>(C<sub>2</sub>O<sub>4</sub>)<sub>3</sub>]<sub>2</sub>[(Cat)<sub>2</sub>[18]crown-6 ether)]·5H<sub>2</sub>O, where M<sup>III</sup> is Cr or Ga (**1** and **2**, respectively) and Cat is H<sub>3</sub>O<sup>+</sup> or NH<sub>4</sub><sup>+</sup>, were synthesized by electrochemical crystallization. Both **1** and **2** crystallized in the triclinic space group (*P* $\bar{1}$ ). From single-crystal X-ray diffraction data recorded at 150 K,<sup>[7]</sup> the structure of the Cr salt has been resolved, with all Cat molecules assigned to H<sub>3</sub>O<sup>+</sup>. X-ray data recorded at 30 K on the Ga salt established the molecular structure, but in addition enabled many of the protons to be resolved.<sup>[8]</sup> The crystal structure consists of successive layers of BEDT-TTF with a  $\beta''$  packing motif (layer A),  $\Delta$ -[(Cat)M(C<sub>2</sub>O<sub>4</sub>)<sub>3</sub>] (layer B), (Cat/H<sub>2</sub>O)-[18]crown-6 (layer C), and  $\Lambda$ -[(Cat)M(C<sub>2</sub>O<sub>4</sub>)<sub>3</sub>] (layer D) arranged in the sequence ...ABCD... (Figure 1). Within experimental error the C–C and C–S bond lengths of the crystallographically inequivalent BEDT-TTF are equal and from the correlation between bond length and charge in BEDT-TTF salts,<sup>[9]</sup> these identify a mean charge on each cation of +0.5, as seen in the  $\beta''$  phase paramagnetic superconductors.

Considering the stoichiometry of **1** and **2** and the known charges of the molecular species, overall charge neutrality requires four monocations (Cat), which could be H<sub>3</sub>O<sup>+</sup> or NH<sub>4</sub><sup>+</sup>. The 30 K structure refinement of **2** confirms the Cat molecules, embedded in the anionic oxalate layers, are all well ordered NH<sub>4</sub><sup>+</sup> ions. In this case there is a marginal improvement in the residual factors for occupancy by nitrogen as compared to oxygen. The remaining cations are predicted to be located in the channels formed by the stack of crown ether molecules. The water molecules found in the channels, refined with a fixed 50% occupancy, form zigzag hydrogen-bonded chains that align with the axis of the crown ether stacks. Additional electron density is located, off the stack axis

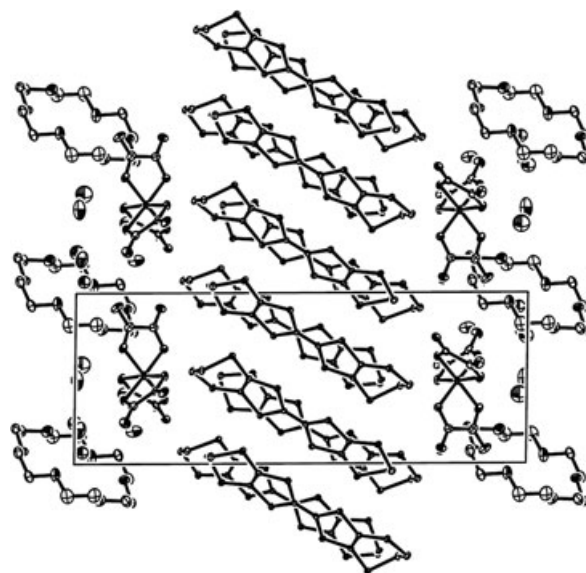


**Figure 1.** The crystal structure of **2** at 30 K, showing the sequence of BEDT-TTF, [(Cat)Ga(C<sub>2</sub>O<sub>4</sub>)<sub>3</sub>], and crown ether layers. Protons have been removed for clarity.

between adjacent crown ether molecules. Refinements were carried out to try to distinguish between the preferred occupancy of these sites as oxygen or as nitrogen atoms, but these refinements were inconclusive. Despite the very low-temperature diffraction data, there is not sufficient information therein to identify individual atomic sites for occupancy by nitrogen or oxygen in these channel regions. Figure 2 shows the zigzag hydrogen-bonded network within the crown ether stacks, with these atoms assigned as oxygen.

Four-probe DC electrical conductivity measurements on single crystals of **1** and **2** with current flow parallel to the layers reveals high electronic conductivities at room temperature (300 Scm<sup>-1</sup> for **1** and 200 Scm<sup>-1</sup> and **2**) with temperature dependence characteristic of a metal. However, in each case the resistance shows an upturn at lower temperature, which occurs at 190 K for **1** and 240 K and **2** (Figure 3). These metal–semiconductor transitions contrast with the behavior of other BEDT-TTF salts of tris(oxalato)metallates, which have metal–superconducting transitions.<sup>[4]</sup>

Measurements of proton conductivity of **1** and **2** from 260–297 K made on pellet samples, show specific conductivities varying from 10<sup>-6</sup> to 10<sup>-3</sup> Scm<sup>-1</sup> over this temperature range (Figure 4a). For each compound the conductivity is activated, as anticipated, but does not follow a simple Arrhenius Law. Instead the measured activation energies change slightly for **1** from 1.06–1.59 eV and for **2** from 1.01–1.92 eV with the lower activation energy at higher temperatures and a gradual change across approximately 280 K. For a similar measurement on Nafion 117 (Figure 4a) there is a constant activation energy of 0.27 eV. A slight discontinuity in protonic conductivity at about 280 K can be seen clearly in Figure 4a for **1** and to a lesser extent for **2**. Typical complex impedance plots are shown for **1** in Figure 4b. The relatively high values of the room-temperature specific conductivity are comparable to those found in polymeric electrolytes of the polyethylene oxide type.<sup>[10]</sup> The mechanism of the proton

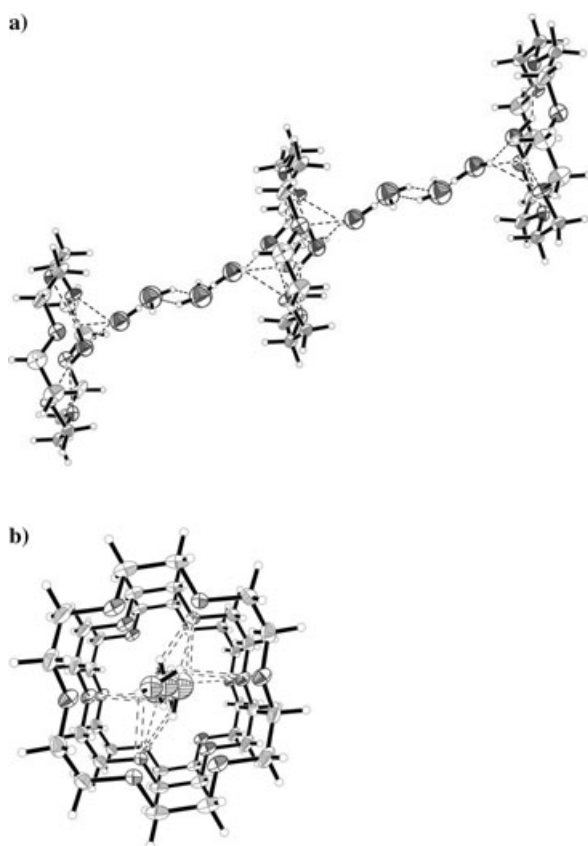


**Figure 2.** Hydrogen-bonding (broken lines) of water molecules within the crown ether stacks of **2** a) perpendicular and b) parallel to the stacks. O black ellipsoids, H small gray circles, C gray ellipsoids.

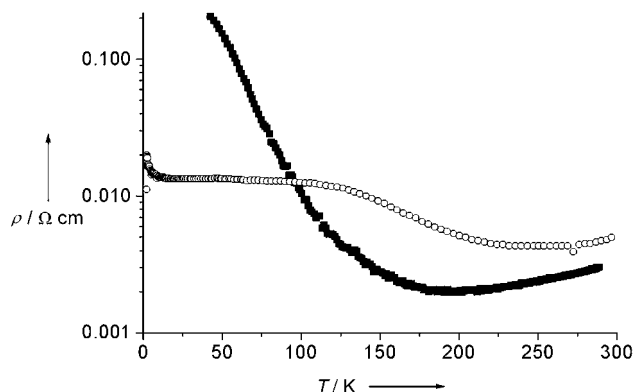


**Figure 3.** Four-probe single-crystal electronic conductivity of **1** (■) and **2** (○).

conductivity is not known. However, it has been established that significant proton conductivity can be mediated by a diffusion mechanism involving  $\text{NH}_4^+/\text{H}_2\text{O}$  or  $\text{NH}_4^+/\text{H}_3\text{O}^+$  species. The former has been found in  $(\text{NH}_4)_4[\text{Fe}(\text{CN})_6] \cdot 1.5\text{H}_2\text{O}$  and the latter in the polytungstate  $(\text{NH}_4)_{10}[\text{W}_{12}\text{O}_{41}] \cdot 5\text{H}_2\text{O}$ ,<sup>[13]</sup> albeit with smaller absolute conductivities than the compounds presented herein.

Solid-state NMR spectra were studied as a function of the temperature in the diamagnetic salt **2**, under magic-angle spinning (MAS) and static conditions. At room temperature, the high-resolution  $^1\text{H}$  spectrum of a fully protonated sample

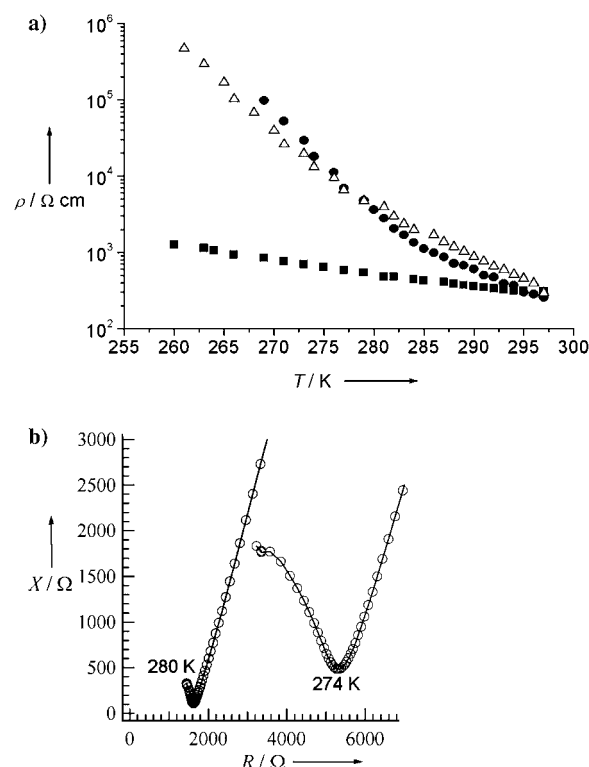


**Figure 4.** a) Proton conductivity of **1** ( $\Delta$ ), **2** ( $\bullet$ ), and Nafion 117 ( $\blacksquare$ ) from 260–297 K with logarithmic y axis; b) typical complex impedance plots for **1** at 274 and 280 K.

consisted of three resonance signals A ( $\delta = 7.7$  ppm), B ( $\delta = 4.3$  ppm), and C ( $\delta = 4.8$  ppm) with intensity ratio 1:0.3: > 2 and widths of 1.6, 0.6, and 7.4 ppm, respectively. Signal A can be assigned to  $\text{H}_2\text{O}$ ,  $\text{H}_3\text{O}^+$  (and/or  $\text{NH}_4^+$ ) since it corresponds to a signal, found in the  $^2\text{H}$  NMR spectrum, which appears when a sample is prepared with  $\text{D}_2\text{O}$ . A separate experiment indicates that the chemical shift of  $\text{ND}_4$  is  $\delta = 7.4$  ppm, similar to the shift of signal A. It is difficult to distinguish between deuterated water and this species since the details of hydrogen bonding, not known from crystallography, could affect the chemical shifts. Signal C is assigned to the  $-\text{CH}_2-$  group of BEDT-TTF and the [18]crown-6 ether. The assignment of signal C is supported by its behavior at low temperature; in the wide-line  $^1\text{H}$  NMR spectrum at 130 K it splits into a doublet with a separation of approximately 30 kHz, which is typical for the nuclear dipole interaction between the two protons in a  $-\text{CH}_2-$  group. Furthermore, the signal is absent in the  $^2\text{H}$  NMR spectrum of the sample when exchanged with  $\text{D}_2\text{O}$ . Signal B, which is much weaker and narrower than the other two, is tentatively assigned to water molecules adsorbed on the surface of the crystallites. The increasing line width of signal C in the wide-line  $^1\text{H}$  NMR spectrum of the fully protonated sample (Figure 5) clearly indicates freezing of the thermal fluctuations of the  $-\text{CH}_2-$  on lowering the temperature. In contrast, the width of signal A, remains relatively constant and small (11 kHz) between 130 and 250 K before decreasing further between 250 and 300 K. The  $^2\text{H}$  NMR spectrum of the  $\text{D}_2\text{O}$  sample further confirms an almost isotropic and rapid rotation of those molecules producing signal A, at least down to 195 K.

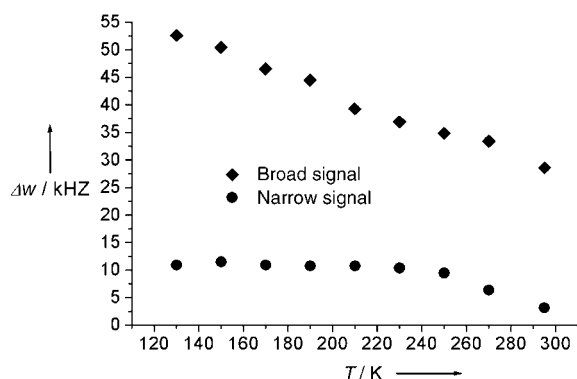


**Figure 5.** Temperature dependence of the spectral width ( $\Delta\omega$ ) of the wide-line  $^1\text{H}$  NMR spectra of a fully  $^1\text{H}$  substituted sample of **2**. The spectral width of BEDT-TTF and [18]crown-6- $\text{CH}_2$ - groups (♦) and of  $\text{H}_2\text{O}$  (●) including the weak signal (signal B, see text) are shown.

In summary, we have identified the first molecular ion-radical salts that are both protonic and metallic conductors. The high values of both the ionic and electronic conductivities at room temperature are especially noteworthy and are attributed to the presence of discrete conducting layers in the crystal consisting of either organosulfur molecules or of crown ether stacks containing disordered  $\text{H}_2\text{O}$ ,  $\text{H}_3\text{O}$ , and/or  $\text{NH}_4$ . This discovery expands the search for other mixed ionic-electronic conductors among the large and versatile family of TTF and BEDT-TTF ion-radical salts.

### Experimental Section

The BEDT-TTF salts were prepared by in situ oxidation of BEDT-TTF (12 mg) in an H-shaped electrochemical cell in the presence of a racemic solution of  $(\text{NH}_4)_3[\text{M}(\text{C}_2\text{O}_4)_3]$  ( $\text{M} = \text{Cr}, \text{Ga}$ ; 120 mg), [18]crown-6-ether (250 mg) and four drops of distilled  $\text{H}_2\text{O}$  in a mixture of freshly distilled  $\text{CH}_3\text{CN}$  (10 mL) and  $\text{CH}_2\text{Cl}_2$  (10 mL). A constant current of 1  $\mu\text{A}$  was applied across the cell and thin dark brown elongated plates of the product grew on the Pt anode in 2–3 days. Elemental analysis calcd (%) for (BEDT-TTF) $_4[(\text{NH}_4)\text{M}(\text{C}_2\text{O}_4)_3]_2[(\text{NH}_4)_2[\text{18}]\text{crown-6}]\cdot 5\text{H}_2\text{O}$ : **1** C 29.58, H 3.18, N 2.16; found: C 29.48, H 2.91, N 1.70; **2** C 29.30, H 2.77, N 2.14; found: C 29.47, H 2.82, N 2.17.

Single-crystal DC conductivity were made using four contacts (15  $\mu\text{m}$  diameter Au wires attached to the crystals with Au paste) and an Oxford Instruments MagLab 2000 cryostat with EP probe.

Temperature-dependent protonic conductivity was measured by the AC impedance method in the frequency range 100– $5 \times 10^6$  Hz using an HP4194A impedance analyzer. The sample, prepared as a compressed pellet with a diameter of 3 mm, was enclosed by a Teflon ring to avoid short circuit; this pellet was then sandwiched by proton-conducting Nafion 117 (Aldrich). The sample was clamped by metal electrodes, and was inserted into a Daikin PS24SS cryogenic refrigerating system. The conductivity was measured in vacuo ( $< 10^{-3}$  torr).

Solid-state high-resolution  $^1\text{H}$  and  $^2\text{H}$  NMR spectra were measured by a magic-angle spinning technique with spinning speed of 25 ( $^1\text{H}$  NMR) and 7 kHz ( $^2\text{H}$  NMR) using a Bruker DSX 300 spectrometer. Echo pulse sequence synchronized with spinning speed was used for ensuring the phase of all spinning side-band signals. The thermometers of the NMR probes were calibrated by standard samples. Wide-line  $^1\text{H}$  NMR spectrum under static conditions was measured by the solid echo pulse sequence  $\pi/2_x - \tau - \pi/2_y$ ; the  $\pi/2$  pulse width and  $\tau$  were 1.5  $\mu\text{s}$  and 15  $\mu\text{s}$ , respectively.

Received: August 17, 2004

**Keywords:** conducting materials · electron transport · ion channels · proton transport

- [1] For example see W. R. M. Kinnon in *Solid State Electrochemistry* (Ed.: P. G. Bruce), Cambridge University, **1994**, pp. 163–178.
- [2] a) T. Akutagawa, T. Hasegawa, T. Nakamura, T. Inabe, G. Saito, *Chem. Eur. J.* **2002**, *8*, 4402–4411; b) T. Akutagawa, S. Takeda, T. Hasegawa, T. Nakamura, *J. Am. Chem. Soc.* **2004**, *126*, 291–294.
- [3] A. E. Goeta, L. K. Thompson, C. L. Sheppard, S. S. Tandon, C. W. Lehmann, J. Cosier, C. Webster, J. A. K. Howard, *Acta Cryst.* **1999**, *C5*, 1243–1246.
- [4] a) M. Kurmoo, A. W. Graham, P. Day, S. J. Coles, M. B. Hursthouse, J. L. Caulfield, J. Singleton, F. L. Pratt, W. Hayes, L. Ducasse, P. Guionneau, *J. Am. Chem. Soc.* **1995**, *117*, 12209–12217; b) S. Rashid, S. S. Turner, P. Day, J. A. K. Howard, P. Guionneau, E. J. L. McInnes, F. E. Mabbs, R. J. H. Clark, S. Firth, T. Biggs, *J. Mater. Chem.* **2001**, *11*, 2095–2101.
- [5] a) L. Martin, S. S. Turner, P. Day, K. M. A. Malik, S. J. Coles, M. B. Hursthouse, *Chem. Commun.* **1999**, 513–514; b) L. Martin, S. S. Turner, P. Day, P. Guionneau, J. A. K. Howard, K. M. A. Malik, M. B. Hursthouse, M. Uruichi, K. Yakushi, *Inorg. Chem.* **2001**, *40*, 1363–1371.
- [6] H. Akutsu, A. Akutsu-Sato, S. S. Turner, P. Day, E. Canadell, S. Firth, R. J. H. Clark, J. Yamada, S. Nakatsuji, *Chem. Commun.* **2004**, *1*, 18–19.
- [7] S. Rashid, S. S. Turner, P. Day, M. E. Light, M. B. Hursthouse, S. Firth, R. J. H. Clark, *Chem. Commun.* **2001**, 1462–1463.
- [8] Crystallographic data for **2**:  $\text{C}_{64}\text{H}_{70}\text{Ga}_2\text{N}_2\text{O}_{37}\text{S}_{32}$ ,  $M_r = 2633.65$ , dark red crystal, crystal size =  $0.3 \times 0.25 \times 0.02 \text{ mm}^3$ , triclinic,  $P\bar{1}$ ,  $a = 10.2070(3)$ ,  $b = 11.2012(3)$ ,  $c = 24.2433(6) \text{ \AA}$ ,  $\alpha = 88.4170(10)^\circ$ ,  $\beta = 24.2433(6)^\circ$ ,  $\gamma = 63.4470(10)^\circ$ ,  $V = 2478.15(12) \text{ \AA}^3$ ,  $Z = 1$ ,  $\rho_{\text{calcd}} = 1.766 \text{ g cm}^{-3}$ ,  $\mu = 1.302 \text{ mm}^{-1}$ , graphite monochromated  $\text{MoK}\alpha$  radiation ( $\lambda = 0.71073 \text{ \AA}$ ),  $T = 30(2) \text{ K}$ , 10910 independent reflections of which 9167 with  $F_0 > 4\sigma(F_0)$  were included in the refinement,  $R_{\text{int}} = 0.026$ , max residual density =  $0.859 \text{ e \AA}^{-3}$ ,  $R_1 = 0.0357$ ,  $wR_2 = 0.0794$ . Data were collected through  $\omega$ -scans, at 30 K, using an Oxford Cryosystems HELIX,<sup>[3]</sup> on a Bruker SMART 1K diffractometer. A numerical absorption correction was applied using SADABS.<sup>[11]</sup> The structure was solved by direct methods and refined using full-matrix least-squares methods (SHELX97),<sup>[12]</sup> with all fully occupied atoms having position and thermal-displacement parameters refined. Hydrogen atoms were placed by Fourier and geometric methods, and refined as riding atoms. Multiple refinements were attempted to definitively determine the cations between adjacent crown ether molecules. The final model was chosen as it give the best residual Fourier map. CCDC-234609 (**2**) contains the supplementary crystallographic data for this paper. These data can be obtained free of charge via [www.ccdc.cam.ac.uk/conts/retrieving.html](http://www.ccdc.cam.ac.uk/conts/retrieving.html) (or from the Cambridge Crystallographic Data Centre, 12 Union Road, Cambridge CB2 1EZ, UK; fax: (+44) 1223-336-033; or deposit@ccdc.cam.ac.uk).
- [9] a) P. Guionneau, C. J. Kepert, D. Chasseau, M. R. Truter, P. Day, *Synth. Met.* **1997**, *86*, 1973–1974; b) P. Guionneau, PhD thesis, Université de Bordeaux I (France), **1996**.
- [10] M. F. Daniel, B. Desbat, J. C. Lassegues, *Solid State Ionics* **1988**, *28–30*, 632.
- [11] G. M. Sheldrick, *SADABS* Empirical absorption correction program, University of Göttingen, Göttingen, **1997**.
- [12] *SHELXTL* version 5.1, Bruker Analytical X-ray instruments, Madison, Wisconsin, U.S.A., **1999**.
- [13] *Proton Conductors, Solids, Membranes and Gels: Materials and Devices* (Ed.: P. Colomban), CUP, Cambridge, **1992**, p. 25.